

Multiscale Global and Regional Feature Learning Using Co-Tuplet Loss for Offline Handwritten Signature Verification

Fu-Hsien Huang and Hsin-Min Lu

Abstract—Handwritten signature verification is a significant biometric verification method widely acknowledged by legal and financial institutions. However, the development of automatic signature verification systems poses challenges due to inter-writer similarity, intra-writer variations, and the limited number of signature samples. To address these challenges, we propose a multiscale global and regional feature learning network (MGRNet) with the co-tuplet loss, a new metric learning loss, for offline handwritten signature verification. MGRNet jointly learns global and regional information from various spatial scales and integrates it to generate discriminative features. Consequently, it can capture overall signature stroke information while detecting detailed local differences between genuine and skilled-forged signatures. To enhance the discriminative capability of our network further, we propose the co-tuplet loss, which simultaneously considers multiple positive and negative examples to learn distance metrics. By dealing with inter-writer similarity and intra-writer variations and focusing on informative examples, the co-tuplet loss addresses the limitations of typical metric learning losses. Additionally, we develop HanSig, a large-scale Chinese signature dataset, to facilitate the development of robust systems for this script. The dataset is available at <https://github.com/ashleyfhh/HanSig>. Experimental results on four benchmark datasets in different languages demonstrate the promising performance of our method in comparison to state-of-the-art approaches.

I. INTRODUCTION

HANDWRITTEN signature verification aims to recognize individuals' signatures for identity verification. This biometric verification approach is commonly accepted by government agencies and financial institutions [1]. The handwritten signature verification systems can be classified into two categories based on the signature acquisition device used: online and offline signature verification. Online verification involves capturing dynamic characteristics of the signing process, such as velocity and pressure, using specialized devices [2]. In contrast, offline verification refers to the static verification

of scanned digital signatures. Since offline verification lacks dynamic characteristics, distinguishing between genuine and forged signatures is inherently more challenging. Moreover, discriminating between genuine signatures and skilled forgeries is difficult due to the high level of imitation similarity (inter-writer similarity). Additionally, practical factors such as significant variations within an individual's signatures (intra-writer variations or intra-personal variability) and the limited number of available signature samples further complicate the implementation of automatic verification systems [3].

Early offline signature verification systems primarily relied on manual feature extraction methods [4], [5]. To address the challenge of intra-writer variations, capturing regional information from local signature regions has been proposed to provide details for static verification [6]–[8]. However, the traditional process involves sequentially applying independent steps of manual regional feature extraction, region similarity estimation, and similarity verification. These methods overlook the interdependencies between feature extraction and similarity measurement, resulting in suboptimal performance. In recent years, some studies [3], [9]–[13] have proposed the adoption of convolutional neural network (CNN)-based metric learning methods to integrate similarity measurement into automatic feature learning, overcoming the limitations of manual feature extraction. However, existing methods either learn from entire signature images or local regions, failing to exploit the complementary nature of global and regional information and limiting the network's ability to learn discriminative features. Additionally, most of these methods trained with typical metric learning losses, such as contrastive loss [14] and triplet loss [15], [16], tend to suffer from slow convergence and bad local minima due to the pair or triplet sampling problem [17], [18].

To overcome the limitations of previous studies, we propose a multiscale global and regional feature learning network (MGRNet) with a new metric learning loss called co-tuplet loss for automatic offline signature verification. MGRNet aims to learn discriminative features from both global and regional contexts to effectively distinguish between genuine and skilled-forged signatures. Learning global representations from the whole image aims to capture the overall information on signature strokes and configuration. However, given the high similarity between genuine signatures and skilled forgeries, it is also necessary to learn regional representations to explore local differences. As illustrated in Fig. 1, the proposed MGRNet starts from a base part and splits into two branches for global and regional feature learning. Unlike

This work was supported in part by National Science and Technology Council of Taiwan (Grants MOST109-2410-H-002-077-MY3 and NSTC112-2410-H-002-087-MY3), and the Center for Research in Econometric Theory and Applications (Grant 112L900203) from the Featured Areas Research Center Program within the framework of the Higher Education Sprout Project by the Ministry of Education in Taiwan, and the National Taiwan University. The authors are extremely grateful for the work of Chia-Chun Ku during the early stages of the research. (*Corresponding author: Hsin-Min Lu.*)

Fu-Hsien Huang is with the Department of Information Management, National Taiwan University, Taipei 106216, Taiwan (e-mail: d10725004@ntu.edu.tw)

Hsin-Min Lu is with the Department of Information Management, and the Center for Research in Econometric Theory and Applications, National Taiwan University, Taipei 106216, Taiwan (e-mail: luim@ntu.edu.tw)

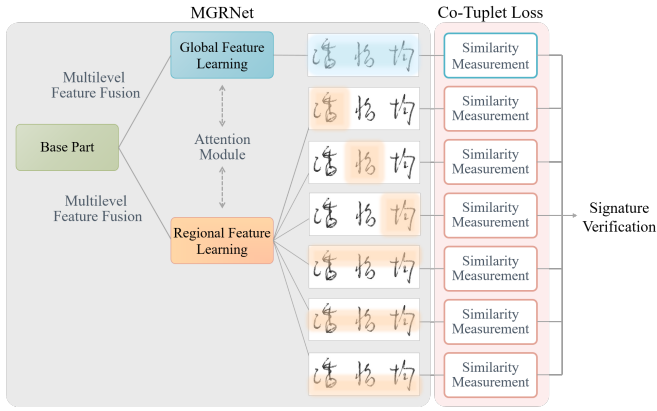


Fig. 1. Illustration of the proposed multiscale global and regional feature learning network (MGRNet) and co-tuplet loss for signature verification.

previous methods, MGRNet simultaneously considers global and regional information in handwritten signatures, dividing deep feature maps into regions to learn local differences. This enables the network to capture information from various spatial scales and integrate it to generate discriminative features. Additionally, we address the thin and sparse nature of signature strokes in images by fusing multilevel features in respective branches, aggregating information learned at different levels. We also introduce an attention module that guides the network to focus on important information by considering interactions between global and regional features. The design of our proposed signature verification system is based on the writer-independent (WI) approach. In contrast to the writer-dependent (WD) approach, WI has the advantages of leveraging information across signatures from different writers and requiring no system updates for new writers.

For global and regional similarity measurement, we propose the co-tuplet loss, a novel metric learning loss, to learn the distance metric for signature verification. The proposed co-tuplet loss aims to transform input features into a feature space where genuine signatures from the same writer are close to each other while corresponding forgeries are far away from genuine ones. Unlike the typical triplet loss [15], [16], the proposed co-tuplet loss simultaneously considers multiple genuine signature examples and multiple forged signature examples to learn similarity metrics. This effectively addresses issues related to intra-writer variability and inter-writer similarity. Additionally, we emphasize the importance of batch construction and example selection to focus the training process on informative examples. It is worth noting that our signature verification system combines the feature learning and similarity measurement steps and can be optimized end-to-end.

For training and evaluation, we utilize four offline handwritten signature datasets in different languages. Three of these datasets are publicly available: CEDAR [19] with English signatures, BHSig-Bengali [20] with Bengali signatures, and BHSig-Hindi [20] with Hindi signatures. To address the lack of large-scale public offline Chinese signature datasets, we create the HanSig dataset, consisting of 35,400 signature samples from 238 writers. Experimental results demonstrate

the promising performance of our proposed MGRNet with co-tuplet loss compared to state-of-the-art methods.

In summary, our contributions can be listed as follows:

- We propose an automatic multiscale feature learning method to generate discriminative features for offline handwritten signature verification. To our best knowledge, this is the first study that adopts deep end-to-end learning to automatically learn both global and regional information and integrate it for signature verification.
- We propose a new metric learning loss function that enhances discriminative capability and facilitates better convergence of our network. The proposed loss enables the training process to pay attention to informative examples and effectively tackles challenges associated with intra-writer signing variation and inter-writer similarity, resulting in improved performance.
- We create the HanSig dataset, a new large-scale offline Chinese signature dataset. Such datasets, which consider writers' signing variations, are crucial for developing robust signature verification systems for this script. Considering that few large-scale Chinese signature datasets are publicly available, we plan to release HanSig to the public to foster future research in this area.

II. RELATED RESEARCH

A. Offline handwritten signature verification

Given the wide use of the offline handwritten signatures, many new approaches for offline signature verification have been developed in the last ten years [21]. Most early work [4], [5] relied on manual feature extraction methods to capture signature stroke variations from signature images. However, the feature extraction process of the traditional methods is easily disturbed by noise, and these methods have a limited capacity to extract complex features [22]. In recent times, there has been a growing interest in utilizing automatic feature extraction methods, particularly CNNs, to learn representations directly from signature images. These methods have effectively overcome the limitations of manual feature extraction. Several studies [23]–[25] employed CNNs as feature extractors, followed by training separate classifiers for forgery detection. Wei *et al.* [26] introduced a four-stream CNN to focus on the sparse stroke information.

For the improvement of offline signature verification, several studies have concentrated on regional information and local details to capture static properties. To address intra-writer variations, Pirlo and Impedovo [6] and Malik *et al.* [7] discovered that stable signature regions exhibit similar patterns among signatures from the same signer. Sharif *et al.* [8] combined global features with local features from 16 image parts. While these methods provided additional information for signature verification, the separation of manual feature extraction and similarity measurement did not guarantee optimal performance. Liu *et al.* [3] proposed a region-based deep learning network that solely used local regions as inputs to obtain signature features.

In contrast to previous works, we propose an offline signature verification system that automatically learns feature

representations from both the entire image and local regions. The combination of global and regional information has demonstrated promise in tasks such as person re-identification [27] and vehicle re-identification [28], which involve training visually similar inter-class samples with intra-class differences. Unlike Liu *et al.* [3], our method combines global and regional information and divides deep feature maps into regions of different sizes. This enables us to aggregate features from multiple scales and improve robustness against misalignment issues. Moreover, our system integrates similarity measurement with feature learning, thereby enhancing the entire training process compared to previous methods [6]–[8], [23]–[25].

B. Metric learning-based methods

Recently, there has been an increased focus on employing metric learning-based methods to learn similarity and dissimilarity for feature representations. The objective of these methods is to learn a good distance metric that transforms input features into a new feature space, where instances belonging to the same class are close together and those from different classes are far apart [29], [30]. Commonly-used metric learning functions for learning pairwise similarities include contrastive loss [14] and triplet loss [15], [16] among others. Deep learning methods that integrate metric learning into feature learning have found wide applications in various domains, including face recognition [31], [32] and person re-identification [30], [33].

In the field of offline handwritten signature systems, metric learning-based methods have also shown promising results. Soleimani *et al.* [29] and Rantzsch *et al.* [9] were among the early researchers who introduced metric learning into signature verification. However, Soleimani *et al.* [29] did not provide a performance comparison with previous works, while Rantzsch *et al.* [9] evaluated the test data used in the training phase. Dey *et al.* [10], Xing *et al.* [11], and Liu *et al.* [3] employed the Siamese network [34] for metric learning. Some studies have proposed improvements to existing metric learning structures to enhance the robustness of offline signature verification. For instance, Maergner *et al.* [12] combined a triplet loss-based CNN with the graph edit distance approach. Wan and Zou [13] and Zhu *et al.* [35] respectively developed a dual triplet loss and a point-to-set (P2S) metric to improve discrimination between genuine signatures and skilled forgeries.

The previous research on handwritten signature verification mainly employed typical metric learning losses or developed improved losses based on similar concepts. However, these losses often suffer from unstable and slow convergence due to inherent sampling problem [17], [18]. To address these limitations of typical metric learning losses, we propose a new metric learning loss. This loss shares similarities with previous tuplet-based losses such as the multi-class N-pair loss [17] and the tuplet margin loss [36]. However, we introduce a unique example selection and mining strategy specifically tailored for the signature verification task to facilitate better convergence.

C. Main public offline signature datasets

According to Hameed *et al.* [22], the GPDS [37], MCVT-75 [38], and CEDAR [19] datasets are among the most commonly

adopted Western signature datasets. Another dataset, SigComp11 [39], contains Dutch and Chinese subsets. UTSig [40] is a frequently used Persian signature dataset. Additionally, the BHSig260 dataset [20] offers two subsets comprising signatures in Bengali and Hindi languages. However, when it comes to offline Chinese handwritten signatures, there is a scarcity of publicly available datasets. Currently, the SigComp2011 [39] and ChiSig [41] datasets are the only existing public datasets for offline Chinese signatures. SigComp2011 has only 1,177 signature samples. In comparison, ChiSig is a new dataset that contains a more substantial number of samples, with a total of 10,242 signatures. While some studies have created offline Chinese signature datasets for their own research purposes [3], [13], [26], these datasets have not been publicly released.

Considering that the characteristics of handwritten signatures differ across languages and scripts due to their unique writing styles [26], it is impractical to train a Chinese signature verification system using Western datasets. Moreover, the development of a realistic signature verification system requires the consideration of signature variability to avoid overfitting [21]. Therefore, we are motivated to create a new offline Chinese signature dataset that contains more samples and incorporates signature variability for each writer.

III. PROPOSED METHOD

In this section, we introduce the multiscale global and regional feature learning network (MGRNet), the handwritten signature verification method proposed in this study. We begin by providing an overview of the overall architecture of MGRNet. Subsequently, we provide a detailed explanation of the proposed network structure. Additionally, we introduce a novel metric learning loss called co-tuplet loss, which aims to improve the discriminative capability of the learned features for signature verification. Finally, we elaborate on the decision-making process in our signature verification system.

A. Overall architecture

Fig. 2 illustrates the overall architecture of MGRNet, which comprises three main components: the base part, the global branch, and the regional branch. To integrate the discriminative signature information of different spatial scales, we propose to automatically learn robust feature representations from both the global and dual-orientation regional branches, which sets it apart from existing methods that rely on manual region feature extraction [6]–[8] and focus solely on local regions [3]. As depicted in Fig. 2, the global and regional branches share a common front base part that consists of several convolutional layers. By jointly optimizing the global and regional branches, we can enhance the feature learning capability of the base part during the training process.

We modify the structure of SigNet-F [23] as the CNN backbone to build our branches and modules. The layers of our CNN backbone are summarized in the supplemental material. We add rectified linear unit (ReLU) activation function and batch normalization (BN) [42] after each convolutional layer to address issues such as vanishing gradients and overfitting during training. Consider a set of genuine signature images from

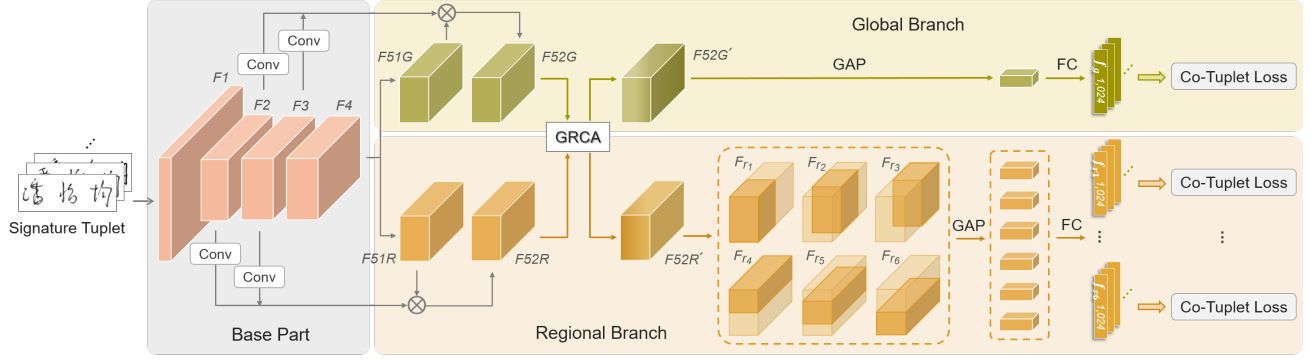


Fig. 2. Overall architecture of MGRNet, which comprises three main components: the base part, the global branch, and the regional branch. We also introduce feature fusion and the global-regional channel attention (GRCA) to facilitate robust global and regional feature learning. Each set of the corresponding features is trained with individual co-tuplet losses.

a specific writer and their corresponding forged counterparts. We refer to this set as a “signature tuplet” in the subsequent discussion. Each input image, denoted as x , belonging to this signature tuplet passes through the base part to sequentially generate the output feature maps, $F1$, $F2$, $F3$, and $F4$. After the Conv4 layer, the network splits into the global and regional branches and learns to generate feature maps $F51G$ and $F51R$ in the respective branches. It is worth noting that our model incorporates multilevel feature fusion and a global-regional channel attention (GRCA) module, which facilitate effective global and regional feature learning, specifically for the signature strokes. Finally, by training each global and regional branch with an individual loss function, we obtain the discriminative global embedding, f_g , and the regional embeddings, f_{r_i} , for $i = 1, \dots, 6$.

B. Multilevel feature fusion

We observed that the signature strokes in the images are thin and sparse compared with general object images. In a typical CNN structure, the low-level features generated from the early layers contain more detailed information. However, information loss of stroke details is inevitable after several convolution and downsampling operators. In order to retain the detailed information of signature strokes for global and regional features, we propose a multilevel feature fusion mechanism that combines low-level features with high-level features and then passes the aggregated information to subsequent layers. Here, the feature maps $F2$ and $F3$ in the base part and the feature maps $F51G$ in the global branch are fused to obtain the feature maps $F52G$. Likewise, $F2$ and $F3$ in the base part and $F51R$ in the regional branch are fused to generate $F52R$. We can express the fusion operations as follows:

$$F52G = \varepsilon^{3 \times 3}(F2) \circ \varepsilon^{3 \times 3}(F3) \circ F51G, \quad (1)$$

$$F52R = \varepsilon^{3 \times 3}(F2) \circ \varepsilon^{3 \times 3}(F3) \circ F51R, \quad (2)$$

where $\varepsilon^{3 \times 3}$ is the convolution operation with a kernel size of 3×3 and a stride of 2 to transfer $F2 \in \mathbb{R}^{C \times H' \times W'}$ and $F3 \in \mathbb{R}^{C' \times H' \times W'}$ to the same shape as $F51G$ and $F51R \in \mathbb{R}^{C \times H \times W}$. The operator \circ denotes the element-wise multiplication.

In contrast to the fusion of only the base part features before splitting into global and regional branches, we propose a different fusion mechanism that utilizes both the global and regional features for their respective branches. Thus, the detailed information of signature strokes can complement to the high-level features in each branch. Instead of the commonly-used concatenation, we employ a multiplicative operation as the fusion strategy. Multiplication has advantages over concatenation as it allows the gradients of each layer to be correlated with the gradients of the other layers during gradient computation [43]. By using multiplication, features at different levels can depend on and interact with each other during the training process. We report ablation studies in the supplemental material to show that multiplication yields better performance compared to concatenation.

C. Global-regional channel attention

In order to extract essential global and regional feature representations, we propose the GRCA module to guide our model in focusing on specific signature information. GRCA simultaneously learns the attention weights for global and regional features by considering their interactions and relative importance. Drawing inspiration from previous attention mechanisms [43], [44], we design GRCA tailored for our two-branch structure to facilitate the signature verification task.

As shown in Fig. 3, we perform global average pooling (GAP) on the feature maps $F52G \in \mathbb{R}^{C \times H \times W}$ in the global branch and $F52R \in \mathbb{R}^{C \times H \times W}$ in the regional branch to compress the spatial information of each channel into one channel descriptor. We obtain two channel descriptors $D1G \in \mathbb{R}^{C \times 1 \times 1}$ and $D1R \in \mathbb{R}^{C \times 1 \times 1}$:

$$D1G^c = \phi(\mathcal{Z}_g^c) = \frac{1}{HW} \sum_{i=1}^H \sum_{j=1}^W \mathcal{Z}_g^c(i, j), \quad (3)$$

$$D1R^c = \phi(\mathcal{Z}_r^c) = \frac{1}{HW} \sum_{i=1}^H \sum_{j=1}^W \mathcal{Z}_r^c(i, j), \quad (4)$$

where ϕ is the GAP operation, \mathcal{Z}_g^c is the c -th channel of $F52G$, and \mathcal{Z}_r^c is the c -th channel of $F52R$, for $c = 1, \dots, C$. For attention map learning, we first use a convolutional layer with a kernel size of 1×1 followed by a ReLU activation function

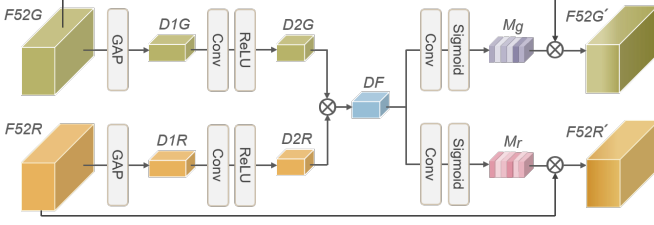


Fig. 3. Detailed structure of the GRCA module. The simultaneous generation of channel-wise attention allows our model to adaptively learn to focus on specific signature information based on the relative importance of global and regional features.

to convert the channel descriptors $D1G$ into $D2G \in \mathbb{R}^{V \times 1 \times 1}$ and $D1R$ into $D2R \in \mathbb{R}^{V \times 1 \times 1}$. We set $V < C$, such that the dimension reduction operation can reduce computational and parameter overhead. Subsequently, we combine $D2G$ and $D2R$ to obtain the fused descriptors $DF \in \mathbb{R}^{V \times 1 \times 1}$ using the multiplicative operation. The fusion of $D2G$ and $D2R$ enables the simultaneous generation of channel-wise attention for both global and regional features. This allows our model to adaptively learn to focus on specific patterns based on the relative importance of global and regional features.

Next, we perform a dimension recovery operation for regional and global branches using convolution with a kernel size of 1×1 , and we obtain the normalized global and regional attention maps M_g and $M_r \in \mathbb{R}^{C \times 1 \times 1}$ using the sigmoid function. The entire process of attention map learning can be expressed as follows:

$$M_g = \sigma(\varepsilon^{1 \times 1}(\gamma(\varepsilon^{1 \times 1}(D1G)) \circ \gamma(\varepsilon^{1 \times 1}(D1R)))), \quad (5)$$

$$M_r = \sigma(\varepsilon^{1 \times 1}(\gamma(\varepsilon^{1 \times 1}(D1G)) \circ \gamma(\varepsilon^{1 \times 1}(D1R)))), \quad (6)$$

where $\varepsilon^{1 \times 1}$ is the convolution operation with a kernel size of 1×1 , γ represents the ReLU function, and σ represents the sigmoid function. We finally multiply each channel of $F52G$ by each weight value of M_g to obtain $F52G' \in \mathbb{R}^{C \times H \times W}$ and perform the same operation on $F52R$ and M_r to obtain $F52R' \in \mathbb{R}^{C \times H \times W}$.

D. Multiscale feature learning

Since genuine and skilled-forged signatures often have only slight differences, previous methods using only global feature learning are insufficient to generate discriminative features for offline signature verification. We propose automatic multiscale feature learning by using both global and regional branches to address the limitations of learning from a single global branch. Here, “multiscale” refers to multiple scales (i.e., sizes) of global and dual-orientation regional feature maps. By learning complementary feature representations from various spatial scales, our method can effectively handle the challenges posed by high inter-writer similarity and intra-writer variations.

1) *Global feature learning*: To capture signature stroke information from the entire image, we first conduct the GAP operation over the feature maps $F52G' \in \mathbb{R}^{C \times H \times W}$ in the global branch, as shown in Fig. 2. Subsequently, we use a fully connected (FC) layer with the output dimension of 1,024 to generate the global embedding f_g for a signature image.

To obtain the final feature representations, instead of using multiple FC layers in the structure proposed in [23] that we use as the CNN backbone, we adopt GAP followed by a single FC layer. This change reduces the model parameters and addresses overfitting issues [45], resulting in improved performance in our experimental evaluations. Additionally, we apply L2-Normalization before the output layer to mitigate the impact of scale variability in the data, which enhances training stability and boosts performance. The process of global feature learning can be formulated as follows:

$$\phi(\mathcal{U}_g^c) = \frac{1}{HW} \sum_{i=1}^H \sum_{j=1}^W \mathcal{U}_g^c(i, j), \quad (7)$$

$$f_g = \eta([\phi(\mathcal{U}_g^1), \phi(\mathcal{U}_g^2), \dots, \phi(\mathcal{U}_g^C)]), \quad (8)$$

where ϕ is the GAP operation, η is the FC layer, and \mathcal{U}_g^c is the c -th channel of $F52G'$, for $c = 1, \dots, C$.

2) *Regional feature learning*: In order to generate discriminative features for signature verification, we propose dual-orientation regional feature learning to complement global feature learning. Rather than using a fixed-sized sliding window along one direction of an input image for region segmentation, we propose to divide the deep feature maps into regions with different scales along both horizontal and vertical orientations. This dual-orientation regional feature learning enables the regional branch to capture more localized differences between genuine and skilled-forged signatures. Our method does not require input segmentation and does not increase the number of model inputs, resulting in improved efficiency, particularly for larger datasets.

Inspired by Pirlo and Impedovo [6], we divide the deep feature maps in the regional branch into three equal-sized vertical regions and three equal-sized horizontal regions. Pirlo and Impedovo [6] conducted segmentation of the input images and analyzed signature stability (i.e., how consistent a writer’s signatures are) for each region using cosine similarity, revealing distinct variability and similarity information in different signature regions. Building upon their insights, we incorporate vertical and horizontal divisions to capture regional information related to signature variations and similarities. We first divide the feature maps $F52R' \in \mathbb{R}^{C \times H \times W}$ into three overlapping vertical regions $F_{r_1}, F_{r_2},$ and $F_{r_3} \in \mathbb{R}^{C \times H \times W''}$ ($W'' < W$) from left to right, as shown in the regional branch of Fig. 2. We also divide the feature maps $F52R'$ into three overlapping horizontal regions $F_{r_4}, F_{r_5},$ and $F_{r_6} \in \mathbb{R}^{C \times H'' \times W}$ ($H'' < H$) from top to bottom, as shown in Fig. 2. To address the potential misalignment of corresponding regions, we make adjacent regions overlap each other, despite the fact that signature images are generally well-aligned and less prone to this issue compared to general object images. The process of region division can be expressed as follows:

$$F_{r_m} = \psi_H(F52R', m), \quad m \in \{1, 2, 3\}, \quad (9)$$

$$F_{r_n} = \psi_V(F52R', n), \quad n \in \{4, 5, 6\}, \quad (10)$$

where ψ_H denotes the feature map division operation in the horizontal orientation, and ψ_V is the same operation in the vertical orientation. Specifically, we empirically set $W'' = 13$

and the overlap between F_{r_m} to be 7 pixels in width, and we empirically set $H'' = 8$ and set the overlap between F_{r_n} to be 4 pixels in height.

Finally, we obtain six regions with varying scales and conduct GAP operations over each of them, followed by an FC layer to generate 1024-dimensional regional embeddings, f_{r_m} , $m \in \{1, 2, 3\}$, and f_{r_n} , $n \in \{4, 5, 6\}$, for each signature image. The process of generating regional embeddings can be formulated as follows:

$$\phi(\mathcal{U}_{r_m}^c) = \frac{1}{HW} \sum_{i=1}^H \sum_{j=1}^{13} \mathcal{U}_{r_m}^c(i, j), \quad (11)$$

$$f_{r_m} = \eta([\phi(\mathcal{U}_{r_m}^1), \phi(\mathcal{U}_{r_m}^2), \dots, \phi(\mathcal{U}_{r_m}^C)]), \quad (12)$$

$$\phi(\mathcal{U}_{r_n}^c) = \frac{1}{HW} \sum_{i=1}^8 \sum_{j=1}^W \mathcal{U}_{r_n}^c(i, j), \quad (13)$$

$$f_{r_n} = \eta([\phi(\mathcal{U}_{r_n}^1), \phi(\mathcal{U}_{r_n}^2), \dots, \phi(\mathcal{U}_{r_n}^C)]), \quad (14)$$

where ϕ is the GAP operation, η is the FC layer, $\mathcal{U}_{r_m}^c$ is the c -th channel of F_{r_m} , and $\mathcal{U}_{r_n}^c$ is the c -th channel of F_{r_n} , for $c = 1, \dots, C$. Similar to the global embedding, we apply L2-Normalization before the output layer for generating regional embeddings. We demonstrate the performance improvement achieved through global and regional feature learning and visualize the differences in their effects in Section IV.

E. Co-tuplet loss

1) *Limitations of typical loss functions:* Previous automatic signature verification methods [10], [12], [13], [23]–[25], [46], [47] have employed the classification loss and the typical metric learning loss to learn similarity measurement. However, the methods trained with the classification loss, such as the categorical cross-entropy loss, can only differentiate between genuine signatures of different writers, limiting their application to random forgery detection or preliminary feature extraction for a WD classifier. In contrast, typical metric learning loss functions such as contrastive loss [14] and triplet loss [15], [16] have been widely integrated into deep learning methods. However, training with a single randomly selected negative example in each update can result in unstable and slow convergence [17], [18]. To address this problem, Sohn [17] extended the concept of a triplet $\{x_a, x_p, x_n\}$ to a tuplet that simultaneously includes more than one negative example: $\{x_a, x_p, x_{n_1}, x_{n_2}, \dots, x_{n_k}\}$, where x_a , x_p , and x_n refer to the anchor, positive, and negative example, respectively, and k is the number of the negative examples in a batch. The tuplet-based loss functions [17], [36] consider multiple negative examples from different classes and aim to increase the inter-class distance by pushing them apart in each update.

In contrast to general object recognition tasks focusing on distinguishing between different classes, handwritten signature verification requires discriminating between positive examples (i.e., genuine signatures) and their corresponding negative examples (i.e., skilled forgeries) within each writer. The challenge lies in the presence of potentially high intra-writer variability in genuine signatures and high inter-writer similarity between genuine and forged signatures. This implies

that the distances between most genuine-genuine pairs may be large, while the distances between genuine-forged pairs tend to be small. Using only one positive example in each update is insufficient for considering the distances of multiple positive examples, thus failing to address the intra-writer distance variation effectively. Similarly, relying on a single negative example in each update does not adequately account for the inter-writer similarity between a positive example and the remaining negative examples.

To address the challenges in handwritten signature verification, we propose a tuplet-based metric learning loss function called the co-tuplet loss. The co-tuplet loss combines the property of tuplet-based loss functions, allowing for the inclusion of multiple negative examples to learn an appropriate distance metric between genuine and forged signatures. Additionally, it employs multiple positive examples, enabling the model to learn the relationship between genuine signatures within each writer, which was previously missing in tuplet-based loss functions [17], [36].

2) *Proposed loss function:* We define a tuplet as $\{x_a, x_{p_1}, x_{p_2}, \dots, x_{p_k}, x_{n_1}, x_{n_2}, \dots, x_{n_k}\}$, where x_a , x_p , and x_n refer to the anchor, positive, and negative examples, respectively. The integer k is the number of positive and negative examples in a mini-batch. In this study, the anchor and positive examples are genuine signatures signed by a writer, while the negative examples are corresponding skilled forgeries. We aim to shorten the intra-writer distance and enlarge the inter-writer distance in the embedding space. To achieve this, we jointly consider the distances of multiple positive and negative examples from the same anchor in the loss function. The formulation of the co-tuplet loss is as follows:

$$\mathcal{L}_{ct} = \log[1 + \sum_{i \in \mathcal{S}(\mathcal{P})} \exp(d_i^+ - d_h^-) + \sum_{j \in \mathcal{S}(\mathcal{N})} \exp(d_h^+ - d_j^-)], \quad (15)$$

where $\mathcal{S}(\mathcal{P})$ and $\mathcal{S}(\mathcal{N})$ are the sets of positive and negative example indices for which the positive and negative examples satisfy our mining strategy described in the next subsection, d indicates the squared Euclidean distance used as the distance metric; and d_i^+ , d_j^- , d_h^+ , and d_h^- are defined as follows:

$$d_i^+ = \|f(x_a) - f(x_{p_i})\|_2^2, \quad (16)$$

$$d_j^- = \|f(x_a) - f(x_{n_j})\|_2^2, \quad (17)$$

$$d_h^+ = \max_{\ell=1 \dots k} \|f(x_a) - f(x_{p_\ell})\|_2^2, \quad (18)$$

$$d_h^- = \min_{\ell=1 \dots k} \|f(x_a) - f(x_{n_\ell})\|_2^2, \quad (19)$$

where $f(\cdot)$ represents the feature embedding of an input example. Among the positive examples in a mini-batch, d_h^+ is the distance between the anchor and the hardest positive example that is the furthest from the anchor. Similarly, among the negative examples in a mini-batch, d_h^- is the distance between the anchor and the hardest negative example that is the closest to the anchor.

The proposed loss comprises two parts, pulling and pushing parts. We design the pulling part to decrease the intra-writer distance by pulling the selected positive examples closer to the anchor using d_h^- as the reference distance. In addition, we use the pushing part to increase the inter-writer distance

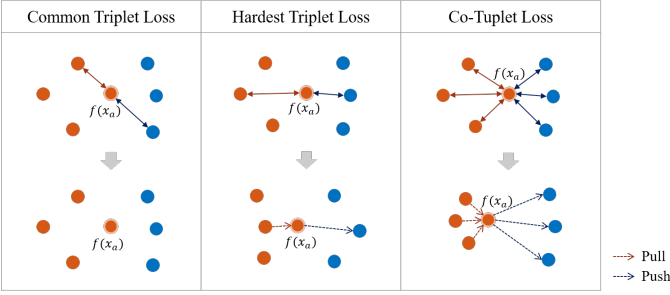


Fig. 4. Example of the distance learning process of the common triplet loss, hardest triplet loss, and co-tuplet loss.

by pushing the selected negative examples farther from the anchor using d_h^+ as the reference distance. Instead of pairwise comparisons between positive and negative examples, we impose penalties on the distances that are larger than the hardest negative example and shorter than the hardest positive example. This reduces the computational complexity from quadratic to linear. Given that the proposed tuplet-based loss relies on the co-existence of multiple positive and negative examples to learn distance metrics, we refer to it as the ‘‘co-tuplet loss.’’

Fig. 4 provides a visual representation of the differences in the distance learning process between the triplet loss, the hardest triplet loss, and the co-tuplet loss. The triplet loss only partially utilizes the distance information of batch examples, as many easy triplets that already satisfy the triplet constraint do not contribute to the training process. Similarly, the hardest triplet loss, which focuses on the hardest positive and negative examples, neglects optimizing the distances from the anchor to the remaining positive and negative examples. In contrast, the proposed co-tuplet loss simultaneously considers multiple positive and negative examples in a mini-batch for distance optimization. This allows the signature verification model to effectively learn to pull genuine signatures belonging to the same writer close together, while pushing forgeries far away from them.

3) Batch construction and constraint mining strategy:

Previous studies have highlighted the significance of batch construction and example selection in loss functions [48]. To construct a training mini-batch, we first randomly select w genuine signatures without replacement as anchor examples. For each anchor, k genuine signatures are randomly sampled (excluding the anchor itself) as positive examples from the same writer. Similarly, k negative examples are randomly sampled from the corresponding forgeries. Together, the anchor, positive examples, and negative examples form a signature tuplet. We repeat this process to generate w tuplets for the training mini-batch.

To select training examples, we propose a constraint mining strategy that focuses the learning process on informative signature examples rather than trivial ones. To the best of our knowledge, this mining strategy is not considered in existing tuplet-based losses [17], [36]. We identify that very easy positive and negative examples still contribute to the loss values in Eq. (15), even though they provide uninformative

and redundant information for embedding learning. Hence, we employ the constraint mining strategy to select informative positive and negative examples for the pulling and pushing parts in Eq. (15), respectively. The selected positive and negative examples must satisfy the following constraints:

$$d_i^+ \geq d_h^- - \delta, \quad (20)$$

$$d_j^- \leq d_h^+ + \delta, \quad (21)$$

where $\delta > 0$ is a constraint margin. Here an appropriate selection of δ ensures that the optimization process does not concentrate on useless information and facilitates our model in learning the accurate mapping of intra-writer and inter-writer distances.

4) *Gradient computation:* We can obtain the gradient of the proposed co-tuplet loss \mathcal{L}_{ct} with respect to the model parameters θ . The gradient computation is provided in the supplemental material along with an observation from the gradient. In comparison to typical metric learning losses, our co-tuplet loss offers the advantage of emphasizing informative examples over uninformative ones by assigning unequal weights to examples based on the distance difference. Since skilled-forged signatures often closely resemble genuine signatures for each writer, this weighting scheme promotes the learning of more discriminative features for handwritten signature verification. The effectiveness of our metric learning loss in signature verification is demonstrated in Section IV.

F. Signature verification decision

In our approach, we train both the global features and the regional features derived from a signature tuplet in an end-to-end manner. We use individual co-tuplet losses to train each set of the corresponding features instead of a single loss for the concatenation of global and regional features. This training strategy enables the model to learn specific information from the global branch and each part of the regional branch. In the supplemental material, we present a comparison between the performance of training with individual losses and training with a single loss. For joint global and regional feature learning, we define the overall objective function as follows:

$$\mathcal{L}_{ct,T} = \mathcal{L}_{ct,g} + \lambda \sum_{i=1}^6 \mathcal{L}_{ct,r_i}, \quad (22)$$

where λ is a hyperparameter used to control the weight of the regional losses.

In the verification stage, namely the test stage, we integrate various spatial information by concatenating the global and regional embeddings into the final embedding for each input image. To make the verification decision, we use a distance threshold d_{thr} to decide whether a given signature pair $\{x_i, x_j\}$ is positive or negative. A positive verification decision indicates that the questioned signature x_j is accepted as genuine with respect to the reference signature x_i . Conversely, x_j with a negative decision is regarded as forged with respect to x_i . We define the final signature verification decision as follows:

$$\text{Decision} = \begin{cases} \text{positive,} & \text{if } d(x_i, x_j) \leq d_{thr} \\ \text{negative,} & \text{if } d(x_i, x_j) > d_{thr}, \end{cases} \quad (23)$$

where $d(x_i, x_j)$ is the squared Euclidean distance between the final embeddings of x_i and x_j .

IV. EXPERIMENTS

In this section, we first describe the benchmark datasets. Following that, we elaborate on the data preprocessing, implementation particulars, and the evaluation metrics used for signature verification. Lastly, we present the experimental results and compare them with various state-of-the-art methods.

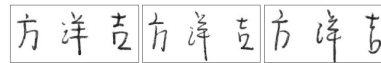
A. Datasets

1) *CEDAR*: The CEDAR dataset [19] consists of English signatures from 55 different writers. Each writer contributed 24 genuine signatures for a specific name and had 24 skilled forgeries generated by forgers. Following previous studies [3], [10], [11], [49], [50], we randomly divide the writers into a training set that includes signatures from 50 writers, and a test set that contains signatures from five writers. We further randomly reserve five writers' signatures from the training set for validation. For each writer in the test set, we use one genuine signature as the reference signature and another genuine signature as the questioned signature to form 276 ($24 \times 23/2$) positive pairs. In addition, we form negative pairs by using one genuine signature as the reference and one forged signature as the questioned signature. To balance the positive and negative pairs, we follow previous studies and randomly select 276 pairs from the negative pairs. The final test data consists of 2,760 signature pairs.

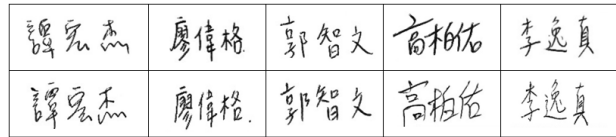
2) *BHSig-Bengali*: The BHSig-Bengali dataset [20] comprises Bengali signatures from 100 different writers. Each writer contributed 24 genuine signatures for a specific name, along with 30 skilled-forged signatures. Following the data splitting scheme in [10], we randomly select signatures from 50 writers to form the training set, while the remaining writers' signatures are used to form the test set. We further reserve five writers' signatures from the training set for validation. Similarly, for each writer in the test set, we form 276 positive pairs and 276 negative pairs. The final test data comprises 27,600 signature pairs.

3) *BHSig-Hindi*: The BHSig-Hindi dataset [20] contains Hindi signatures from 160 writers. Each writer contributed 24 genuine signatures for a specific name, accompanied by 30 skilled-forged signatures. Consistent with previous studies [10], [51], we randomly select signatures from 100 writers to form the training set, while the remaining writers' signatures are used for the test set. Within the training set, we randomly select signatures from five writers to create the validation set. For each writer in the test set, we follow a similar procedure to generate 276 positive pairs and 276 negative pairs. The final test data comprises 33,120 signature pairs.

4) *HanSig*: Due to the scarcity of large-scale public offline Chinese signature datasets, we construct the HanSig signature dataset to be made publicly available and to facilitate the development of signature verification systems. We generated 885 candidate names based on the frequency distributions of the name distribution in the real world. By generating candidate names, we took precautions to avoid potential legal concerns



(a) Examples of collected signatures in three styles



(b) Examples of collected genuine and forged signatures

Fig. 5. Examples of signature images in HanSig. The left, middle, and right images of (a) are the collected signatures written in neat, normal, and stylish styles, respectively. The first row of (b) shows the collected genuine signatures, and the second row of (b) shows the corresponding forged signatures.

related to personal information. We collected signatures of these candidate names from 238 writers. To introduce more signing variations, each name was signed 20 times in three different styles: neat, normal, and stylish. We provide the details of our dataset collection process in the supplemental material. Overall, HanSig consists of a total of 17,700 genuine signatures and an equal number of skilled forgeries. Fig. 5 provides examples of the collected signatures in different styles and the genuine and forged signatures.

The HanSig dataset has several valuable characteristics. Firstly, the generation of names for signatures addresses concerns regarding personal information and privacy while still preserving the distributional characteristics of real names. Secondly, HanSig incorporates the real-world property of intra-writer variability by including multiple signature styles. Moreover, HanSig surpasses existing public Chinese signature datasets in terms of the number of signature samples, providing robust training for signature verification systems. Lastly, HanSig is advantageous for both random and skilled forgery verification tasks.

We randomly split HanSig into a training set and a test set. The training set comprises 795 names signed by 213 writers, while the test set includes 90 names signed by 25 writers. From the training set, 20 writers' signatures (78 names) are randomly selected for validation. For each name in the test set, we follow a similar procedure used in the CEDAR and BHSig to form 190 positive pairs and 190 negative pairs. The final test data of HanSig consists of 34,200 signature pairs.

B. Data preprocessing

To mitigate the influence of background and position variations in the signature images, we perform several data preprocessing steps without deforming the structure of the signatures. Firstly, we convert the signature images to grayscale. Next, we apply Otsu's algorithm [52] to transform all background pixel values into 255 while keeping the signature pixels unchanged. This step removes noise in image backgrounds and is critical to datasets (e.g., CEDAR) that have distinct backgrounds in genuine and forged signature images. We also center-crop the signature images and remove the excess blanks around the signatures to eliminate potential misalignment issues caused by signature position variations. Finally, the images are resized to the input size of the network using bilinear interpolation,

and the pixel values of the signature images are normalized to a range between 0 and 1. The examples of images before and after these preprocessing steps are displayed in the supplemental material.

C. Implementation details and evaluation metrics

In our model, we experimentally set $C = 256$, $H = 16$, $W = 25$, and $V = 32$. We construct a training mini-batch using $w = 18$ for CEDAR, HanSig, and BHSig-Bengali and $w = 20$ for BHSig-Hindi. Furthermore, we set $k = 5$ for all datasets. The constraint margin δ for the constraint mining strategy is empirically set as 0.2 for CEDAR and 0.3 for HanSig, BHSig-Bengali, and BHSig-Hindi. In our experiments, we empirically set $\lambda = 1$ in the objective function as the weight of the regional losses. We apply Adam optimizer [53] with an initial learning rate of 0.001, and the learning rate decays by a factor of 0.5 every 15 epochs. We train our models for a maximum of 80 epochs and use the validation set for early stopping. All our experiments are implemented using the PyTorch framework.

We report the performance using the common evaluation metrics of signature verification: False Reject Rate (FRR), False Accept Rate (FAR), Equal Error Rate (EER), and Area Under the Curve (AUC). FRR refers to the proportion of genuine signatures mistakenly rejected as forgeries. FAR is the proportion of forgeries mistakenly accepted as genuine signatures. The values of FRR and FAR vary with the adjustment of the decision threshold d_{thr} . We report FRR and FAR under d_{thr} that maximizes the accuracy. EER is the error rate when FRR is equal to FAR. The calculations of EER and AUC are independent of the selection of d_{thr} .

D. Method evaluation and analysis

To assess the performance of the proposed MGRNet combined with the co-tuplet loss, we conduct experiments comparing it to a simple baseline model and alternative combinations of losses and models. The evaluation aims to determine the effectiveness of the co-tuplet loss compared to the triplet loss [15], [16] and to understand the relative performance of the MGRNet. As a simple baseline, we adopt a VGG-16 [54] pretrained on the ImageNet dataset [55] as the feature extractor. Additionally, we train the MGRNet with the triplet loss and evaluate its performance for the comparison with the co-tuplet loss. Furthermore, alternative combinations include training the VGG-16 with either the co-tuplet loss or the triplet loss under the same experimental settings.

Table I reports the experimental results. The MGRNet trained with the co-tuplet loss achieves the best performance across all datasets. Compared to the simple baseline, it improves the EER by up to 19.57 percentage points and improves the AUC by up to 15.44 percentage points. Replacing the co-tuplet loss with the triplet loss for training the MGRNet results in worsened EER and AUC. Similarly, training the VGG-16 with the co-tuplet loss yields better performance in terms of EER and AUC compared to training it with the triplet loss. Furthermore, comparing the MGRNet to the VGG-16 trained with the same loss function, the MGRNet consistently

outperforms the VGG-16 counterparts. When trained with the co-tuplet loss and the triplet loss, the MGRNet exhibits EER improvements ranging from 5.33 to 12.94 and from 5.15 to 11.01 percentage points over the VGG-16, respectively. Overall, the results validate the effectiveness of the MGRNet coupled with the co-tuplet loss across different datasets.

E. Ablation studies

In this subsection, we conduct ablation studies to evaluate the validity of selected operations and the importance of each module/branch in our network. Considering the length limitation, we present the results of validity of selected operations in the supplemental material. To assess the contribution of each module/branch in our proposed MGRNet, we remove specific components from the original framework. Specifically, we remove multilevel feature fusion, GRCA, global branch, and regional branch, and evaluate the impacts on signature verification performance. The results of these ablation studies are reported in Table II.

The findings indicate that removing multilevel feature fusion results in performance degradation across all datasets, especially with a reduction of 3.23 percentage points for CEDAR. This suggests that our proposed fusion mechanism effectively mitigates information loss caused by layer transmission and retains detailed signature stroke information for both global and regional branches. Additionally, the GRCA module demonstrates a performance improvement ranging from 0.28 to 1.27 percentage points. This highlights the effectiveness of our attention mechanism in focusing on important channel information, enabling the model to learn salient features.

We further examine the importance of the global and regional branches in our proposed approach. The results in Table II indicate that both the global and regional branches contribute to enhancing signature verification performance. The global branch provides more performance gains for CEDAR, while the regional branch makes a greater contribution to the other datasets. These results suggest that both global and regional feature learning are crucial for exploiting their respective advantages. The global branch can capture the overall signature stroke information without being affected by misalignment issues. In contrast, the regional branch focuses on learning the detailed differences, capturing additional information and further boosting performance.

F. Visualization analysis

1) *Comparison between extracted features:* We compare the 2D projections of extracted features from the simple baseline (pretrained VGG-16), MGRNet with triplet loss, and MGRNet with co-tuplet loss using the t-distributed stochastic neighbor embedding (t-SNE) algorithm [56]. To ensure clarity, we use signatures from a randomly selected subset of 50 names out of the 90 names in the HanSig test set. Fig. 6 (a) displays the feature space projection of the simple baseline. It shows that genuine and corresponding forged signatures of each name are clustered together. For instance, the red solid circle highlights a cluster from a single name where genuine signatures are visually inseparable from forged signatures

TABLE I
PERFORMANCE COMPARISON BETWEEN DIFFERENT COMBINATIONS OF MODELS AND LOSSES (EVALUATION METRICS IN %)

Dataset	Method	FRR	FAR	EER	AUC
CEDAR	Simple Baseline (Pretrained VGG-16)	16.67	27.75	23.08	84.82
	VGG-16 with triplet loss	17.32	18.48	17.93	87.62
	VGG-16 with co-tuplet loss	17.90	15.00	16.45	90.15
	MGRNet with triplet loss	7.75	5.94	6.92	98.10
	MGRNet with co-tuplet loss	3.55	3.33	3.51	99.47
BHSig-Bengali	Simple Baseline (Pretrained VGG-16)	11.71	22.23	17.04	91.07
	VGG-16 with triplet loss	12.70	12.63	12.69	94.80
	VGG-16 with co-tuplet loss	14.44	9.08	11.96	95.75
	MGRNet with triplet loss	9.41	5.21	7.54	98.03
	MGRNet with co-tuplet loss	6.20	5.93	6.12	98.64
BHSig-Hindi	Simple Baseline (Pretrained VGG-16)	17.28	17.71	17.52	90.64
	VGG-16 with triplet loss	14.05	15.63	14.94	92.74
	VGG-16 with co-tuplet loss	11.91	15.94	14.04	93.86
	MGRNet with triplet loss	9.16	8.58	8.9	96.94
	MGRNet with co-tuplet loss	6.56	6.76	6.68	98.28
HanSig	Simple Baseline (Pretrained VGG-16)	32.43	19.66	26.31	80.94
	VGG-16 with triplet loss	15.60	22.40	19.07	89.47
	VGG-16 with co-tuplet loss	14.20	16.21	15.26	92.60
	MGRNet with triplet loss	9.99	10.82	10.44	95.92
	MGRNet with co-tuplet loss	7.69	11.85	9.93	96.38

TABLE II

ABLATION STUDY TO EVALUATE THE SIGNATURE VERIFICATION PERFORMANCE WITHOUT EACH MODULE/BRANCH IN THE PROPOSED FRAMEWORK (EER IN %). VALUES IN THE PARENTHESES INDICATE THE PERFORMANCE DEGRADATION (EER INCREASE IN %) COMPARED WITH USING EACH MODULE/BRANCH

without Module/Branch	CEDAR	BHSig-Bengali	BHSig-Hindi	HanSig
Multilevel feature fusion	6.74 (3.23)	7.29 (1.17)	9.84 (3.16)	11.02 (1.09)
GRCA	4.78 (1.27)	6.59 (0.47)	6.96 (0.28)	10.48 (0.55)
Global branch	6.70 (3.19)	7.34 (1.22)	7.19 (0.51)	10.70 (0.77)
Regional branch	5.14 (1.63)	8.26 (2.14)	10.85 (4.17)	10.76 (0.83)

represented by “o” and “x” marks, respectively. A similar pattern is observed for another name within the red dashed circle. This suggests that the simple baseline can differentiate between signatures of different names, distinguishing genuine signatures from random forgeries, but it struggles to separate genuine signatures from skilled forgeries in most cases.

Fig. 6 (b) presents the feature space of MGRNet trained with the triplet loss. It demonstrates a better separation between genuine and forged signatures compared to the simple baseline. However, some genuine signatures and their corresponding forgeries remain clustered together. For example, the two red dashed circles indicate separate genuine and forged signatures of a name, while the red solid circle shows that genuine and forged signatures are visually indistinguishable. Additionally, the triplet loss fails to pull genuine signatures of each name closer together. Fig. 6 (c) illustrates the feature space of MGRNet trained with the co-tuplet loss. It shows visually separable clusters of genuine and forged signatures

for each name. The two red solid circles highlight separate clusters of genuine and forged signatures for one name, while the two red dashed circles indicate a similar pattern for another name. Compared to the baseline and the model trained with the triplet loss, MGRNet trained with the co-tuplet loss exhibits improved separation between genuine and forged signatures. These experimental results demonstrate the promising generalization ability of our proposed MGRNet with the co-tuplet loss to unseen data.

2) *Comparison between global and regional branches:* To highlight the benefits of global and regional feature learning, we provide visual explanations of the convolutional layers in both the global and regional branches. We generate heat maps using Grad-CAM [57], [58] for two genuine signature images and their corresponding forgeries from the test sets of BHSig-Bengali and HanSig. Fig. 7 displays the results obtained from Conv51G and Conv51R (the first convolutional layers of the global and regional branches).

Conv51G exhibits attention to various areas of the entire image, capturing overall signature information such as outlines and stroke configuration. In comparison, Conv51R focuses more on signature strokes and highlights local details in specific signature regions. For instance, it emphasizes sharp curves in the upper region of the BHSig-Bengali images and slanting lines in the lower region of the HanSig images. Moreover, Conv51R emphasizes both small details (e.g., the end of a vertical line in genuine signatures of BHSig-Bengali) and larger detailed parts (e.g., the entire vertical line in forged signatures of BHSig-Bengali), enabling the model to learn fine-grained differences between signatures. These visualization results indicate that the global and regional branches have distinct focuses and capture different yet complementary signature information. Integrating information obtained from multiple spatial scales allows for the generation of more

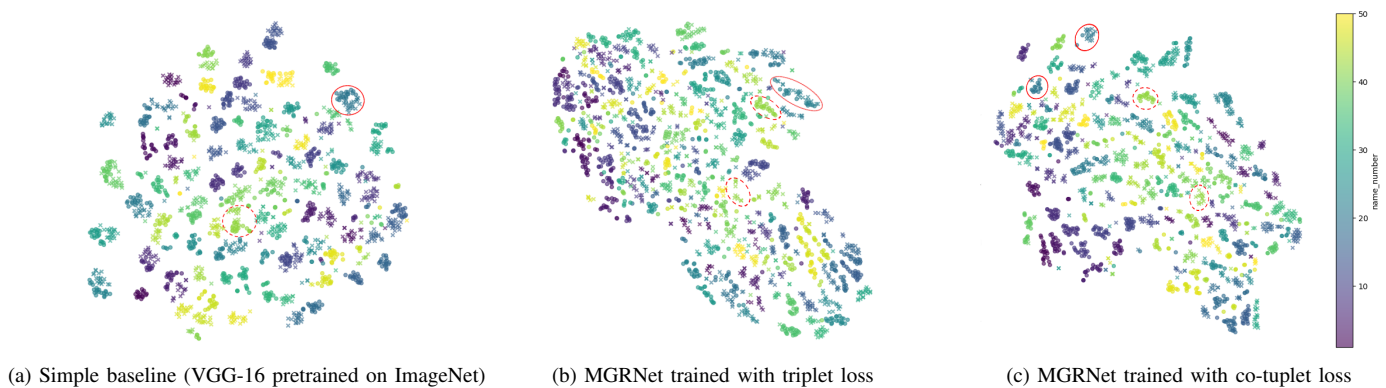


Fig. 6. 2D projections of the extracted features of the random 50 names (each name has 20 genuine and 20 skilled-forged signature images) from the HanSig test set using t-SNE [56]. Each marker represents a signature sample: “o” represents the genuine signatures, and “x” represents the forged signatures. The signature samples belonging to different names are displayed in different colors. The red solid circle and dashed circle indicate the samples of the two names.

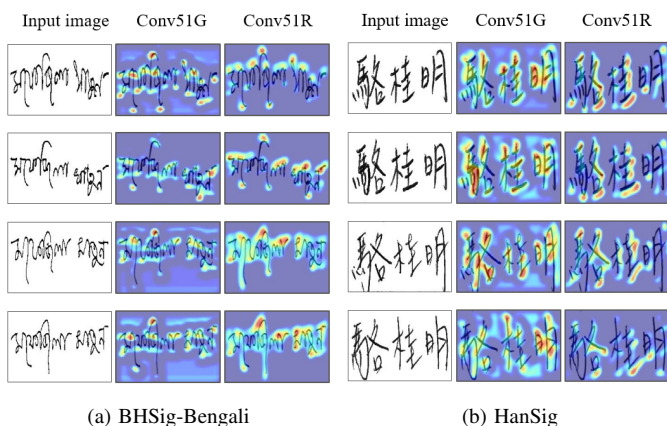


Fig. 7. Visualizing the convolutional layer of the global branch and the regional branch using Grad-CAM [57]. The images in the first column are the input images. The top two and bottom two images are genuine signatures and the corresponding skilled forgeries, respectively, from the test set of BHSig-Bengali and HanSig. The visualization results generated from Conv51G and Conv51R are shown in the second and third columns.

discriminative features in signature verification.

G. Performance comparison with state-of-the-art methods

We present a comparison between our proposed method and several state-of-the-art methods on the three public datasets. For our newly created HanSig, we provide results of several baseline methods for comparison under the same experimental settings. Note that previous works might report different metrics for their methods. To ensure comparability across different studies, we primarily focus on metrics that do not require threshold setting, namely EER and AUC. In cases where previous works only report Average Error Rate (AER), the average of FRR and FAR, which is considered to be comparable to EER [3]. We also provide additional information about each compared method. Additionally, we present a comparison of the number of parameters between our MGRNet and several deep networks in the supplemental material.

1) *Comparison on CEDAR*: Table III demonstrates that our MGRNet with the co-tuplet loss achieves superior performance compared to other methods on CEDAR. Our method outperforms OC-SVM [59], graph-based CNN [12], P2S metric

[35], Siamese network [11], and MSDN [3], which also employ metric learning for signature verification. Notably, our approach surpasses MSDN [3], which solely utilizes local regions from input segmentation for feature learning. This result highlights the efficacy of our proposed multiscale feature learning. It is important to mention that certain previous works did not perform noise removal of the image background during data preprocessing, as mentioned in [3]. However, the image backgrounds of genuine and forged signatures in CEDAR exhibit significant differences, which could lead to overestimated performance. Therefore, Table III excludes works that reported a 0% error rate without background removal.

2) *Comparison on BHSig-Bengali*: Table IV highlights the notable performance improvement of our proposed MGRNet with the co-tuplet loss on BHSig-Bengali compared to state-of-the-art methods. Our method surpasses SigNet [10], SURDS [47], and DeepHSV [51] by 7.77, 6.54, and 5.8 percentage points in terms of EER, respectively. These three methods incorporate typical metric learning losses such as contrastive loss [14] and triplet loss [15], [16] for signature verification. In contrast, our proposed tuplet-based metric learning loss enhances the discriminative power of the learned features, leading to improved performance.

3) *Comparison on BHSig-Hindi*: Table V demonstrates the substantial performance improvement of our proposed MGRNet with the co-tuplet loss compared to previous methods on BHSig-Hindi. Among the WI methods, our method achieves an EER of 6.68%, which is significantly lower than the EERs of SigNet [10] (15.36%), SURDS [47] (10.50%), and DeepHSV [51] (13.34%). This comparison with other state-of-the-art methods showcases the competitiveness and effectiveness of our proposed approach.

4) *Comparison on HanSig*: Since HanSig is a newly-created dataset, we compare the proposed method against three baselines on this dataset. The first baseline is SigNet [10], which utilizes a Siamese network architecture for offline signature verification. We use the provided source code from the author and ensure that the data subsets used for SigNet are consistent with our method. The second and third baselines are VGG-16 [54] and ResNet-18 [60] pretrained on the ImageNet dataset [55], respectively. As depicted in Table VI,

TABLE III

COMPARISON WITH EXISTING METHODS ON THE CEDAR DATASET (EVALUATION METRICS IN %). TYPE REFERS TO THE WD OR WI APPROACH. #REF INDICATES THE NUMBER OF GENUINE SIGNATURES AS THE REFERENCES FOR THE QUESTIONED SIGNATURE TO BE COMPARED WITH. METRIC REFERS TO WHETHER METRIC LEARNING IS USED FOR MODEL TRAINING, WITH “Y” INDICATING YES AND “N” INDICATING NO. “*” REFERS TO AER WHEN FRR EQUALS FAR; HENCE, IT IS THE SAME AS EER. “**” REFERS TO AER, BUT FRR AND FAR ARE OF UNEQUAL VALUE

Method	Type	#Ref	Metric	EER	AUC
Genetic algorithm [8]	WD	12	N	4.67*	-
SigNet-F [23]	WD	12	N	4.63	-
OC-SVM [59]	WD	12	Y	5.60**	-
Graph-based CNN [12]	WI	10	Y	12.27	-
P2S metric [35]	WI	5	Y	9.29	-
Morphology [49]	WI	1	N	11.59	-
Surroundedness [50]	WI	1	N	8.33*	-
Siamese network [11]	WI	1	Y	8.50	-
MSDN [3]	WI	1	Y	6.74	-
MGRNet+co-tuplet loss (Ours)	WI	1	Y	3.51	99.47

TABLE IV

COMPARISON WITH EXISTING METHODS ON THE BHSIG-BENGALI DATASET (EVALUATION METRICS IN %)

Method	Type	#Ref	Metric	EER	AUC
Texture features [20]	WD	12	N	33.82	-
Micro deformations [46]	WD	8	N	8.21	-
Duplication model [61]	WD	2	N	10.67	95.30
SigNet [10]	WI	1	Y	13.89*	-
SURDS [47]	WI	1	Y	12.66**	-
DeepHSV [51]	WI	1	Y	11.92	95.50
MGRNet+co-tuplet loss (Ours)	WI	1	Y	6.12	98.64

our proposed method demonstrates superior performance on HanSig when compared to the three baseline methods.

V. CONCLUSION

In this study, we propose a multiscale feature learning network and a new metric learning loss to build an automatic handwritten signature verification system. The proposed multi-scale global and regional feature learning network (MGRNet) captures complementary signature information from multiple spatial scales. It can integrate the information to generate discriminative features for static signature verification. The multilevel feature fusion and global-regional channel attention (GRCA) modules designed for the two-branch structure provide further performance gains. To enhance the discriminative capability of our verification system, we propose the co-tuplet loss, a novel metric learning loss function. Experimental results demonstrate that our MGRNet with the co-tuplet loss surpasses the state-of-the-art methods on various benchmark datasets, showcasing its effectiveness in signature verification across different languages. While our results are promising, further improvements could be made by developing alternative methods to integrate global and regional signature information.

REFERENCES

[1] A. K. Jain, A. Ross, and S. Prabhakar, “An introduction to biometric recognition,” *IEEE Trans. Circuits Syst. Video Technol.*, vol. 14, no. 1, pp. 4–20, 2004.

TABLE V

COMPARISON WITH EXISTING METHODS ON THE BHSIG-HINDI DATASET (EVALUATION METRICS IN %)

Method	Type	#Ref	Metric	EER	AUC
Texture features [20]	WD	12	N	24.47	-
Micro deformations [46]	WD	8	N	9.01	-
Duplication model [61]	WD	2	N	11.88	94.15
SigNet [10]	WI	1	Y	15.36*	-
SURDS [47]	WI	1	Y	10.50**	-
DeepHSV [51]	WI	1	Y	13.34	94.00
MGRNet+co-tuplet loss (Ours)	WI	1	Y	6.68	98.28

TABLE VI

COMPARISON WITH BASELINE METHODS ON THE HANSIG DATASET (EVALUATION METRICS IN %)

Method	FRR	FAR	EER	AUC
SigNet [10]	32.43	19.66	26.31	80.94
Pretrained VGG-16 [54]	19.18	36.92	28.86	78.34
Pretrained ResNet-18 [60]	27.57	37.05	32.42	73.77
MGRNet+co-tuplet loss (Ours)	7.69	11.85	9.93	96.38

- [2] M. A. Khan, M. K. K. Niazi, and M. A. Khan, “Velocity-image model for online signature verification,” *IEEE Trans. Image Process.*, vol. 15, no. 11, pp. 3540–3549, 2006.
- [3] L. Liu, L. Huang, F. Yin, and Y. Chen, “Offline signature verification using a region based deep metric learning network,” *Pattern Recognit.*, vol. 118, p. 108009, 2021.
- [4] J. Vargas, M. Ferrer, C. Travieso, and J. B. Alonso, “Off-line signature verification based on grey level information using texture features,” *Pattern Recognit.*, vol. 44, no. 2, pp. 375–385, 2011.
- [5] G. Pirlo and D. Impedovo, “Verification of static signatures by optical flow analysis,” *IEEE Trans. Hum.-Mach. Syst.*, vol. 43, no. 5, pp. 499–505, 2013.
- [6] —, “Cosine similarity for analysis and verification of static signatures,” *IET Biom.*, vol. 2, no. 4, pp. 151–158, 2013.
- [7] M. I. Malik, M. Liwicki, A. Dengel, S. Uchida, and V. Frinken, “Automatic signature stability analysis and verification using local features,” in *Proc. 14th Int. Conf. Front. Handwrit. Recognit.*, Hersonissos, Greece, 2014, pp. 621–626.
- [8] M. Sharif, M. A. Khan, M. Faisal, M. Yasmin, and S. L. Fernandes, “A framework for offline signature verification system: Best features selection approach,” *Pattern Recognit. Lett.*, vol. 139, pp. 50–59, 2020.
- [9] H. Rantzsch, H. Yang, and C. Meinel, “Signature embedding: Writer independent offline signature verification with deep metric learning,” in *Proc. 12th Int. Symp. Vis. Comput.*, vol. 10073, Las Vegas, NV, USA, 2016, pp. 616–625.
- [10] S. Dey, A. Dutta, J. I. Toledo, S. K. Ghosh, J. Lladós, and U. Pal, “Signet: Convolutional siamese network for writer independent offline signature verification,” 2017, *arXiv:1707.02131*.
- [11] Z.-J. Xing, F. Yin, Y.-C. Wu, and C.-L. Liu, “Offline signature verification using convolution Siamese network,” in *Proc. Int. Conf. Graph. Image Process.*, vol. 10615, Qingdao, China, 2018, p. 1061511.
- [12] P. Maergner, V. Pondenkandath, M. Alberti, M. Liwicki, K. Riesen, R. Ingold, and A. Fischer, “Combining graph edit distance and triplet networks for offline signature verification,” *Pattern Recognit. Lett.*, vol. 125, pp. 527–533, 2019.
- [13] Q. Wan and Q. Zou, “Learning metric features for writer-independent signature verification using dual triplet loss,” in *Proc. 25th Int. Conf. Pattern Recognit.*, Milan, Italy, 2021, pp. 3853–3859.
- [14] R. Hadsell, S. Chopra, and Y. LeCun, “Dimensionality reduction by learning an invariant mapping,” in *Proc. IEEE Conf. Comput. Vis. Pattern Recognit. (CVPR)*, vol. 2, New York, NY, USA, 2006, pp. 1735–1742.
- [15] M. Schultz and T. Joachims, “Learning a distance metric from relative comparisons,” in *Proc. Adv. Neural Inf. Process. Syst. (NIPS)*, vol. 16, Whistler, BC, Canada, 2003, pp. 41–48.
- [16] K. Q. Weinberger and L. K. Saul, “Distance metric learning for large margin nearest neighbor classification,” *J. Mach. Learn. Res.*, vol. 10, no. 2, pp. 207–244, 2009.
- [17] K. Sohn, “Improved deep metric learning with multi-class n-pair loss

- objective,” in *Proc. Adv. Neural Inf. Process. Syst. (NIPS)*, vol. 29, Barcelona, Spain, 2016, pp. 1857–1865.
- [18] X. Wang, X. Han, W. Huang, D. Dong, and M. R. Scott, “Multi-similarity loss with general pair weighting for deep metric learning,” in *Proc. IEEE/CVF Conf. Comput. Vis. Pattern Recognit. (CVPR)*, Long Beach, CA, USA, 2019, pp. 5017–5025.
- [19] M. K. Kalera, S. Srihari, and A. Xu, “Offline signature verification and identification using distance statistics,” *Int. J. Pattern Recognit. Artif. Intell.*, vol. 18, no. 07, pp. 1339–1360, 2004.
- [20] S. Pal, A. Alaei, U. Pal, and M. Blumenstein, “Performance of an offline signature verification method based on texture features on a large Indic-script signature dataset,” in *Proc. 12th IAPR Int. Work. Doc. Anal. Syst.*, Santorini, Greece, 2016, pp. 72–77.
- [21] M. Diaz, M. A. Ferrer, D. Impedovo, M. I. Malik, G. Pirlo, and R. Plamondon, “A perspective analysis of handwritten signature technology,” *ACM Comput. Surv.*, vol. 51, no. 6, pp. 1–39, 2019.
- [22] M. M. Hameed, R. Ahmad, M. L. M. Kiah, and G. Murtaza, “Machine learning-based offline signature verification systems: A systematic review,” *Signal Process. Image Commun.*, vol. 93, p. 116139, 2021.
- [23] L. G. Hafemann, R. Sabourin, and L. S. Oliveira, “Learning features for offline handwritten signature verification using deep convolutional neural networks,” *Pattern Recognit.*, vol. 70, pp. 163–176, 2017.
- [24] L. G. Hafemann, L. S. Oliveira, and R. Sabourin, “Fixed-sized representation learning from offline handwritten signatures of different sizes,” *Int. J. Doc. Anal. Recognit.*, vol. 21, no. 3, pp. 219–232, 2018.
- [25] S. Bonde, P. Narwade, and R. Sawant, “Offline signature verification using convolutional neural network,” in *Proc. IEEE Int. Conf. Signal Process. Comput.*, Noida, India, 2020, pp. 119–127.
- [26] P. Wei, H. Li, and P. Hu, “Inverse discriminative networks for handwritten signature verification,” in *Proc. IEEE/CVF Conf. Comput. Vis. Pattern Recognit. (CVPR)*, Long Beach, CA, USA, 2019, pp. 5764–5772.
- [27] G. Wang, Y. Yuan, J. Li, S. Ge, and X. Zhou, “Receptive multi-granularity representation for person re-identification,” *IEEE Trans. Image Process.*, vol. 29, pp. 6096–6109, 2020.
- [28] X. Liu, S. Zhang, X. Wang, R. Hong, and Q. Tian, “Group-group loss-based global-regional feature learning for vehicle re-identification,” *IEEE Trans. Image Process.*, vol. 29, pp. 2638–2652, 2019.
- [29] A. Soleimani, B. N. Araabi, and K. Fouladi, “Deep multitask metric learning for offline signature verification,” *Pattern Recognit. Lett.*, vol. 80, pp. 84–90, 2016.
- [30] Y. Zhao, C. Shen, X. Yu, H. Chen, Y. Gao, and S. Xiong, “Learning deep part-aware embedding for person retrieval,” *Pattern Recognit.*, vol. 116, p. 107938, 2021.
- [31] J. Hu, J. Lu, and Y.-P. Tan, “Discriminative deep metric learning for face verification in the wild,” in *Proc. IEEE Conf. Comput. Vis. Pattern Recognit. (CVPR)*, Columbus, OH, USA, 2014, pp. 1875–1882.
- [32] F. Schroff, D. Kalenichenko, and J. Philbin, “FaceNet: A unified embedding for face recognition and clustering,” in *Proc. IEEE Conf. Comput. Vis. Pattern Recognit. (CVPR)*, vol. 1, Boston, MA, USA, 2015, pp. 815–823.
- [33] H. Ye, H. Liu, F. Meng, and X. Li, “Bi-directional exponential angular triplet loss for RGB-infrared person re-identification,” *IEEE Trans. Image Process.*, vol. 30, pp. 1583–1595, 2020.
- [34] J. Bromley, I. Guyon, Y. LeCun, E. Säckinger, and R. Shah, “Signature verification using a “Siamese” time delay neural network,” in *Proc. Adv. Neural Inf. Process. Syst. (NIPS)*, vol. 6, Denver, CO, USA, 1993, p. 737–744.
- [35] Y. Zhu, S. Lai, Z. Li, and L. Jin, “Point-to-set similarity based deep metric learning for offline signature verification,” in *Proc. 17th Int. Conf. Front. Handwrit. Recognit.*, Dortmund, Germany, 2020, pp. 282–287.
- [36] B. Yu and D. Tao, “Deep metric learning with triplet margin loss,” in *Proc. IEEE/CVF Int. Conf. Comput. Vis. (ICCV)*, Seoul, Korea, 2019, pp. 6490–6499.
- [37] M. A. Ferrer, M. Diaz-Cabrera, and A. Morales, “Static signature synthesis: A neuromotor inspired approach for biometrics,” *IEEE Trans. Pattern Anal. Mach. Intell.*, vol. 37, no. 3, pp. 667–680, 2015.
- [38] J. Ortega-García, J. Fierrez-Aguilar, D. Simon, J. Gonzalez, M. Faundez-Zanuy, V. Espinosa, A. Satue, I. Hernaez, J.-J. Igarza, and C. Vivaracho, “MCYT baseline corpus: A bimodal biometric database,” *IEE Proc.-Vis. Image Signal Process.*, vol. 150, no. 6, pp. 395–401, 2003.
- [39] M. Liwicki, M. I. Malik, C. E. Van Den Heuvel, X. Chen, C. Berger, R. Stoel, M. Blumenstein, and B. Found, “Signature verification competition for online and offline skilled forgeries (SigComp2011),” in *Proc. Int. Conf. Doc. Anal. Recognit. (ICDAR)*, Beijing, China, 2011, pp. 1480–1484.
- [40] A. Soleimani, K. Fouladi, and B. N. Araabi, “UTSig: A Persian offline signature dataset,” *IET Biom.*, vol. 6, no. 1, pp. 1–8, 2016.
- [41] K. Yan, Y. Zhang, H. Tang, C. Ren, J. Zhang, G. Wang, and H. Wang, “Signature detection, restoration, and verification: A novel Chinese document signature forgery detection benchmark,” in *Proc. IEEE/CVF Conf. Comput. Vis. Pattern Recognit. (CVPR)*, New Orleans, LA, USA, 2022, pp. 5163–5172.
- [42] S. Ioffe and C. Szegedy, “Batch normalization: Accelerating deep network training by reducing internal covariate shift,” in *Proc. Int. Conf. Mach. Learn.*, vol. 37, Lille, France, 2015, pp. 448–456.
- [43] J. Wei, Q. Wang, Z. Li, S. Wang, S. K. Zhou, and S. Cui, “Shallow feature matters for weakly supervised object localization,” in *Proc. IEEE/CVF Conf. Comput. Vis. Pattern Recognit. (CVPR)*, Nashville, TN, USA, 2021, pp. 5989–5997.
- [44] X. Qin, Z. Wang, Y. Bai, X. Xie, and H. Jia, “FFA-Net: Feature fusion attention network for single image dehazing,” in *Proc. 34th AAAI Conf. Artif. Intell.*, vol. 34, New York, NY, USA, 2020, pp. 11908–11915.
- [45] M. Lin, Q. Chen, and S. Yan, “Network in network,” 2013, *arXiv:1312.4400*.
- [46] Y. Zheng, B. K. Iwana, M. I. Malik, S. Ahmed, W. Ohyama, and S. Uchida, “Learning the micro deformations by max-pooling for offline signature verification,” *Pattern Recognit.*, vol. 118, p. 108008, 2021.
- [47] S. Chattopadhyay, S. Manna, S. Bhattacharya, and U. Pal, “SURDS: Self-supervised attention-guided reconstruction and dual triplet loss for writer independent offline signature verification,” in *Proc. 26th Int. Conf. Pattern Recognit.*, Montreal, QC, Canada, 2022, pp. 1600–1606.
- [48] C.-Y. Wu, R. Manmatha, A. J. Smola, and P. Krahenbuhl, “Sampling matters in deep embedding learning,” in *Proc. IEEE Int. Conf. Comput. Vis. (ICCV)*, Venice, Italy, 2017, pp. 2840–2848.
- [49] R. Kumar, L. Kundu, B. Chanda, and J. Sharma, “A writer-independent off-line signature verification system based on signature morphology,” in *Proc. Int. Conf. Intell. Interact. Technol. Multimed. (IITM)*, New York, NY, USA, 2010, pp. 261–265.
- [50] R. Kumar, J. Sharma, and B. Chanda, “Writer-independent off-line signature verification using surroundedness feature,” *Pattern Recognit. Lett.*, vol. 33, no. 3, pp. 301–308, 2012.
- [51] C. Li, F. Lin, Z. Wang, G. Yu, L. Yuan, and H. Wang, “DeepHSV: User-independent offline signature verification using two-channel CNN,” in *Proc. Int. Conf. Doc. Anal. Recognit. (ICDAR)*, Sydney, NSW, Australia, 2019, pp. 166–171.
- [52] N. Otsu, “A threshold selection method from gray-level histograms,” *IEEE Trans. Syst. Man Cybern. Syst.*, vol. 9, no. 1, pp. 62–66, 1979.
- [53] D. P. Kingma and J. Ba, “Adam: A method for stochastic optimization,” in *Proc. Int. Conf. Learn. Represent. (ICLR)*, San Diego, CA, USA, 2015, pp. 1–15.
- [54] K. Simonyan and A. Zisserman, “Very deep convolutional networks for large-scale image recognition,” in *Proc. Int. Conf. Learn. Represent. (ICLR)*, San Diego, CA, USA, 2015.
- [55] J. Deng, W. Dong, R. Socher, L.-J. Li, K. Li, and L. Fei-Fei, “ImageNet: A large-scale hierarchical image database,” in *Proc. IEEE Conf. Comput. Vis. Pattern Recognit. (CVPR)*, Miami, FL, USA, 2009, pp. 248–255.
- [56] L. Van der Maaten and G. Hinton, “Visualizing data using t-SNE,” *J. Mach. Learn. Res.*, vol. 9, pp. 2579–2605, 2008.
- [57] R. R. Selvaraju, M. Cogswell, A. Das, R. Vedantam, D. Parikh, and D. Batra, “Grad-CAM: Visual explanations from deep networks via gradient-based localization,” *Int. J. Comput. Vis.*, vol. 128, no. 2, pp. 336–359, 2020.
- [58] J. Gildenblat. (2021) *PyTorch Library for CAM Methods*. [Online]. Available: <https://github.com/jacobgil/pytorch-grad-cam>
- [59] Y. Guerbaï, Y. Chibani, and B. Hadjadji, “The effective use of the one-class SVM classifier for handwritten signature verification based on writer-independent parameters,” *Pattern Recognit.*, vol. 48, no. 1, pp. 103–113, 2015.
- [60] K. He, X. Zhang, S. Ren, and J. Sun, “Deep residual learning for image recognition,” in *Proc. IEEE Conf. Comput. Vis. Pattern Recognit. (CVPR)*, Las Vegas, NV, USA, 2016, pp. 770–778.
- [61] M. Diaz, M. A. Ferrer, and R. Sabourin, “Approaching the intra-class variability in multi-script static signature evaluation,” in *Proc. 23rd Int. Conf. Pattern Recognit.*, Cancun, Mexico, 2016, pp. 1147–1152.

Multiscale Global and Regional Feature Learning Using Co-Tuplet Loss for Offline Handwritten Signature Verification

Supplemental Material

I. OVERVIEW

In this supplemental material, we first present the CNN backbone of the proposed MGRNet. Then we provide the gradient computation of our proposed co-tuplet loss. After that, we describe the collection process of our newly created HanSig dataset, followed by displaying examples before and after data preprocessing. Finally, we evaluate the validity of the selected operations and show that our backbone and MGRNet are parameter-efficient compared to several deep networks.

II. LAYERS OF OUR CNN BACKBONE

The layers of our CNN backbone used to build the branches and modules of the MGRNet are summarized in TABLE I.

TABLE I

SUMMARY OF OUR CNN BACKBONE. EXCEPT FOR THE FULLY CONNECTED LAYER, ALL SIZES ARE DESCRIBED IN $DEPTH \times HEIGHT \times WIDTH$

Layer	Size	Stride & Padding
Input	$1 \times 150 \times 220$	
Convolution (Conv1)	$96 \times 11 \times 11$	Stride = 1, pad = 0
Pooling	$96 \times 3 \times 3$	Stride = 2
Convolution (Conv2)	$256 \times 5 \times 5$	Stride = 1, pad = 2
Pooling	$256 \times 3 \times 3$	Stride = 2
Convolution (Conv3)	$384 \times 3 \times 3$	Stride = 1, pad = 1
Convolution (Conv4)	$384 \times 3 \times 3$	Stride = 1, pad = 1
Convolution (Conv5)	$256 \times 3 \times 3$	Stride = 1, pad = 1
Pooling	$256 \times 3 \times 3$	Stride = 2
Global average pooling (GAP)	$256 \times 1 \times 1$	
Fully connected (FC)	1,024	

III. GRADIENT COMPUTATION OF CO-TUPLET LOSS

We can obtain the gradient of the proposed co-tuplet loss with respect to the model parameters θ . The gradient computation is as follows:

$$\begin{aligned} \frac{\partial \mathcal{L}_{ct}}{\partial \theta} &= \frac{1}{q} \left[\sum_{i \in \mathcal{S}(\mathcal{P})} \exp(d_i^+ - d_h^-) \frac{\partial (d_i^+ - d_h^-)}{\partial \theta} \right. \\ &\quad \left. + \sum_{j \in \mathcal{S}(\mathcal{N})} \exp(d_h^+ - d_j^-) \frac{\partial (d_h^+ - d_j^-)}{\partial \theta} \right] \\ &\equiv \frac{1}{q} \left[\sum_{i \in \mathcal{S}(\mathcal{P})} w_{1,i} \frac{\partial (d_i^+ - d_h^-)}{\partial \theta} \right. \\ &\quad \left. + \sum_{j \in \mathcal{S}(\mathcal{N})} w_{2,j} \frac{\partial (d_h^+ - d_j^-)}{\partial \theta} \right], \quad (1) \end{aligned}$$

where

$$q = 1 + \sum_{i \in \mathcal{S}(\mathcal{P})} \exp(d_i^+ - d_h^-) + \sum_{j \in \mathcal{S}(\mathcal{N})} \exp(d_h^+ - d_j^-), \quad (2)$$

and $w_{1,i}$ and $w_{2,j}$ denote the weights of the pulling and pushing parts, respectively. As observed from the above gradient, both $w_{1,i}$ and $w_{2,j}$ are exponentially up-weighted with hard examples and exponentially down-weighted with easy ones.

In comparison to typical metric learning losses, our co-tuplet loss offers the advantage of emphasizing informative examples over uninformative ones by assigning unequal weights to examples based on the distance difference in $d_i^+ - d_h^-$ and $d_h^+ - d_j^-$. Since skilled-forged signatures often closely resemble genuine signatures for each writer, this weighting scheme promotes the learning of more discriminative features for handwritten signature verification. Furthermore, our proposed loss function takes into account moderate examples (i.e., the examples of normal cases) for distance learning. As a result, it avoids overweighting extremely hard examples, leading to a more stable optimization process.

IV. DATA COLLECTION PROCESS OF HANSIG

Due to the scarcity of large-scale public offline Chinese signature datasets, we construct the HanSig dataset to be made publicly available and to facilitate the development of signature verification systems. To begin, we collected 554,723 names from the Joint College Entrance Exam admissions lists between 1996 and 2002. These names were further divided into first names and last names, and we filtered out the first and last names that appeared less than two times. Next, we generated 885 candidate names based on the frequency distributions of the first and last names to match the name distribution in the real world. By generating candidate names,

we took precautions to avoid potential legal concerns related to personal information.

To create genuine signatures, we assigned the previously generated candidate names to 238 writers. Each writer was allocated either three or six candidate names and asked to sign each name 20 times. To introduce more variations in the genuine signatures, we requested each writer to sign each candidate name in three different styles: neat, normal, and stylish. The genuine signatures were subsequently passed on to another writer, referred to as the forger, to create forged signatures. Because this study aims to distinguish between genuine signatures and skilled forgeries, we requested the forgers to practice and skillfully imitate the genuine signatures to create forged signatures. Overall, the HanSig dataset consists of a total of 35,400 signature samples (17,700 genuine signatures and an equal number of skilled forgeries).

V. EXAMPLES OF DATA PREPROCESSING

Fig. 1 displays examples of CEDAR before and after the data preprocessing steps (excluding the last step of normalization of pixel values). This figure shows that removing noise in image backgrounds is critical to datasets (e.g., CEDAR) that have distinct backgrounds in genuine and forged signature images.

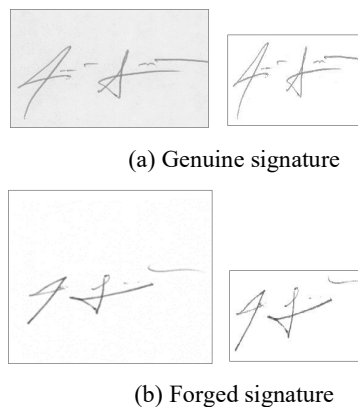


Fig. 1. Examples of CEDAR before and after preprocessing. The left images of (a) and (b) are original signature images, and the right images are preprocessed results.

VI. ABLATION STUDY - VALIDITY OF SELECTED OPERATIONS

To evaluate the validity of the selected operations for multilevel feature fusion and model training, we compare the signature verification performances on CEDAR using different operations while maintaining the same experimental settings. The results of this comparison are presented in TABLE II. Regarding multilevel feature fusion, the original “multiplication” is compared with the conventional “concatenation” as the fusion strategy for combining low-level and high-level features. The results demonstrate that using “multiplication” leads to a significant improvement in EER by 4.32 percentage points compared to using “concatenation.”

This indicates the superiority of the multiplicative operation, which promotes interaction between low-level and high-level features during training and contributes to enhanced performance.

For model training, the original approach involves training each set of global and regional features with individual couplet losses, which enforces the model to learn specific global and regional information. In contrast, an alternative approach is employed where the features are concatenated and trained with only one loss during the learning process. The results in TABLE II reveal that training “with individual losses” outperforms training “with only one loss” by 5.04 percentage points. This suggests that training with individual losses allows the model to learn more discriminative representations and leads to improved signature verification performance.

TABLE II
PERFORMANCE COMPARISON BETWEEN DIFFERENT OPERATIONS ON CEDAR (EER IN %)

	Operation	EER
Multilevel feature fusion	Concatenation	7.83
	Multiplication (Ours)	3.51
Model training	With only one loss	8.55
	With individual losses (Ours)	3.51

VII. COMPARISON OF THE NUMBER OF PARAMETERS

The backbone of our handwritten signature verification system consists of only five convolutional layers and one FC layer, which is more parameter-efficient than the very deep networks, such as VGGNet [1], ResNet [2], and DenseNet [3], as shown in TABLE III. This makes our MGRNet more lightweight than existing signature verification systems based on these deep networks [4]–[7]. Our MGRNet that requires less computation complexity can be easily trained on small signature datasets to achieve competitive performance, even without pretraining on large datasets.

TABLE III
COMPARISON OF THE NUMBER OF LEARNABLE PARAMETERS. ALL METHODS ARE SET TO HAVE THE SAME OUTPUT DIMENSION OF 1,024

Method	#Params
CNN Backbone	
VGG-16 [1]	117.48M
ResNet-18 [2]	11.69M
DenseNet-121 [3]	8.00M
Ours	3.99M
MGRNet (Ours)	7.96M

REFERENCES

- [1] K. Simonyan and A. Zisserman, "Very deep convolutional networks for large-scale image recognition," in *Proc. Int. Conf. Learn. Represent. (ICLR)*, San Diego, CA, USA, 2015.
- [2] K. He, X. Zhang, S. Ren, and J. Sun, "Deep residual learning for image recognition," in *Proc. IEEE Conf. Comput. Vis. Pattern Recognit. (CVPR)*, Las Vegas, NV, USA, 2016, pp. 770–778.
- [3] G. Huang, Z. Liu, L. Van Der Maaten, and K. Q. Weinberger, "Densely connected convolutional networks," in *Proc. IEEE Conf. Comput. Vis. Pattern Recognit. (CVPR)*, Honolulu, HI, USA, 2017, pp. 2261–2269.
- [4] L. Liu, L. Huang, F. Yin, and Y. Chen, "Offline signature verification using a region based deep metric learning network," *Pattern Recognit.*, vol. 118, p. 108009, 2021.
- [5] P. Maergner, V. Pondenkandath, M. Alberti, M. Liwicki, K. Riesen, R. Ingold, and A. Fischer, "Combining graph edit distance and triplet networks for offline signature verification," *Pattern Recognit. Lett.*, vol. 125, pp. 527–533, 2019.
- [6] S. Bonde, P. Narwade, and R. Sawant, "Offline signature verification using convolutional neural network," in *Proc. IEEE Int. Conf. Signal Process. Comput.*, Noida, India, 2020, pp. 119–127.
- [7] S. Chattopadhyay, S. Manna, S. Bhattacharya, and U. Pal, "SURDS: Self-supervised attention-guided reconstruction and dual triplet loss for writer independent offline signature verification," in *Proc. 26th Int. Conf. Pattern Recognit.*, Montreal, QC, Canada, 2022, pp. 1600–1606.